J. Physiol. (1976), **254**, *pp.* 427–454
With 18 *text-figures*
Printed in Great Britain

AN ELECTROPHYSIOLOGICAL STUDY OF CHEMICAL AND ELECTRICAL SYNAPSES ON NEURONES IN THE PARASYMPATHETIC CARDIAC GANGLION OF THE MUDPUPPY, *NECTURUS MACULOSUS*: EVIDENCE FOR INTRINSIC GANGLIONIC INNERVATION

BY S. ROPER*

From the Department of Neurobiology, Harvard Medical School, Boston, Massachusetts 02115, U.S.A.

(*Received 9 April 1975*)

SUMMARY

1. The cardiac ganglion of the mudpuppy is situated on a thin sheet of tissue. Two nerve cell types can be distinguished readily in the living preparation – principal cells and smaller interneurones which synapse with the principal cells. The purpose of this study was to investigate synaptic transmission and the functional organization of neuronal connexions of ganglion cells with intracellular micro-electrodes.

2. Stimulation of the preganglionic, vagus, nerves evoked a large excitatory response in principal cells. About three quarters of these neurones were innervated by a single vagal axon. The remaining cells received two or more preganglionic nerve fibres.

3. The quantum content of vagal excitatory post-synaptic potentials (e.p.s.p.s) was measured. Normally, the e.p.s.p. was suprathreshold and consisted of about twenty-two quanta, whereas only about nine quanta were required to reach threshold and initiate an action potential.

4. Intracellular stimulation of principal cells evoked e.p.s.p.s in neighbouring principal cells. The responses were blocked by cholinergic antagonists. These potentials were caused by excitation of principal cell axon collateral synapses.

5. Principal cells also formed electrical junctions with each other. These electrical junctions were very weak. Although they transmitted slow potential changes, only a small response was recorded in one cell when an electrically coupled neighbouring cell fired an impulse. The resistance of the electrical junction between principal cells was calculated to be about $5–8 \times 10^8\ \Omega$.

* Present address: Department of Anatomy, University of Colorado Medical Center, 4200 East Ninth Avenue, Denver, Colorado 80220, U.S.A.

6. Stable penetrations of interneurones were only rarely achieved, making it difficult to study their functional relationship to principal cells. Action potentials were recorded from interneurones in a few instances.

7. These data demonstrate that parasympathetic ganglion cells in the heart of the mudpuppy receive innervation from more than one source involving both chemical and electrical synapses, and that some of the synapses are intrinsic to the ganglion.

INTRODUCTION

Our understanding of synaptic transmission has been greatly increased by investigation of autonomic ganglia and the neuromuscular junction of skeletal muscle fibres where it is possible to recognize the region of the synapses on living cells and to impale individual cells with micro-electrodes (McMahan & Kuffler, 1971; McMahan, Spitzer & Peper, 1972). These preparations have been valuable for studying many fundamental properties of the transmission of nerve impulses at chemical synapses, and have contributed considerable information about the release and action of neurotransmitters (see Katz, 1969; Dennis, Harris & Kuffler, 1971).

The innervation of skeletal muscle fibres and some autonomic ganglia – notably, the parasympathetic ganglion in the heart of the frog (McMahan & Kuffler, 1971) – is characterized by a single or very few nerve endings of one type, namely cholinergic. One would like to extend these studies of synaptic transmission to cells where heterogeneous synaptic inputs interact and where single cells and their synaptic endings could also be recognized in the living state.

This report presents results of a study of synaptic transmission in a new preparation which combines these features. In the preceding paper (McMahan & Purves, 1976) a description was given of the preparation, the cardiac ganglion of the mudpuppy, *Necturus maculosus*. In the isolated living ganglion individual neurones, their processes and their synapses can be seen. Moreover, there are catecholamine-containing interneurones within the ganglion which synapse with the principal neurones. These interneurones resemble the small, intensely fluorescent (SIF) neurones found in autonomic ganglia from other animals (e.g. Matthews & Raisman, 1969; Jacobowitz, 1970). In addition, McMahan & Purves (1976) present morphological evidence for both electrical and chemical synaptic contacts which link one principal cell directly to another.

In this paper, the functional organization of the ganglion and some of the properties of the chemical and electrical synaptic inputs have been studied with intracellular micro-electrode recordings. In the following paper (Roper, 1976) the effects of removing one of the sources of innerva-

tion on the post-synaptic chemosensitivity and the remaining synapses is evaluated.

METHODS

The experiments were done on *Necturus maculosus* (mudpuppies, 20–30 cm long). Animals were obtained fresh from the supplier and kept in cold tanks (5° C) of 5 % Ringer solution until used.

Dissection. Animals were killed by decapitation and the heart was exposed. The cardiac ganglion lies between the large hepatic veins at their entrance into the sinus venosus (see McMahan & Purves, 1976). The entire heart, along with the ganglion, was pinned out in a small dissecting dish containing frog Ringer or 80 % Leibovitz culture medium (supplemented with $CaCl_2$ to a final concentration of 2–4 mM). The heart and surrounding tissue were carefully cut away from the ganglion and the ganglion transferred to a small chamber designed to fit under a 40 × water immersion objective (cf. McMahan & Kuffler, 1971). Micro-electrodes were manipulated beneath the objective under direct visual control and using differential interference contrast optics.

Recording techniques. Micro-electrodes for intracellular recording were pulled from glass capillary tubing which contained a few fine glass fibres. The electrodes were boiled in 2·5 M-KCl and left overnight at 5° C to fill. KCl-filled micro-electrodes were inspected at 400 × magnification and only those with an even taper and tips below the resolution of the light microscope were selected. The micro-electrodes used in these experiments had resistances of 100–400 MΩ.

Micro-electrodes were connected by way of fine silver–silver chloride wires to high-input impedance amplifiers having a negative capacitance-compensation circuit and including a Wheatstone bridge arrangement to allow passage of current through the electrode while recordings were being made.

Current was monitored by keeping the bath at virtual ground potential with a feed-back circuit utilizing an operational amplifier. The non-inverting input of the operational amplifier was grounded and the inverting input attached to a silver–silver chloride wire in contact with the solution in the chamber. The output of the operational amplifier was fed back to the inverting input via a 10^7 Ω resistor, and current flow was monitored across this resistance.

Stimulation. The cut end of the post-ganglionic nerve was drawn into a small suction electrode in order to stimulate ganglion cells antidromically. Similarly, the distal stumps of both preganglionic nerves (vagi) were drawn into separate suction electrodes. In this manner, cells could be excited either antidromically by post-ganglionic stimulation or synaptically by preganglionic stimulation.

RESULTS

General description of principal cells and interneurones

When the sheet of tissue with the ganglion was stretched out in the recording chamber and viewed with the compound microscope, two types of nerve cells could be distinguished clearly – large principal cells (30–50 μm in diameter) which innervate the cardiac muscle and smaller 'multipolar' interneurones (McMahan & Purves, 1976).

Membrane properties of principal cells. When the principal cells were penetrated with micro-electrodes, the resting membrane potentials were

typically 45–55 mV, and rarely greater than 60 mV. Small depolarizing currents injected intracellularly usually evoked overshooting impulses (Fig. 1*A*). However, the peak amplitude of the action potential was reduced by losses introduced by the high resistance electrodes.

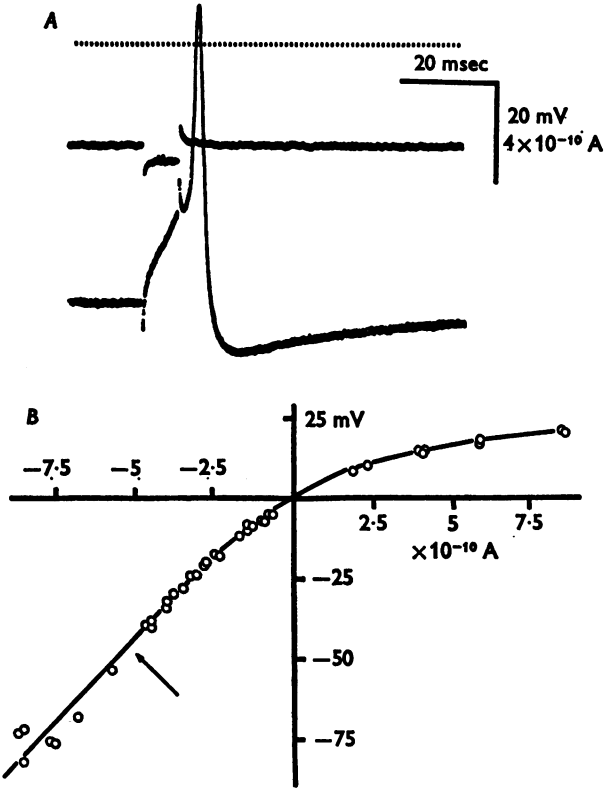

Fig. 1. Active and passive membrane characteristics of the principal cells in the mudpuppy ganglion (the records are from two different cells). *A*, overshooting action potential (bottom trace) generated by a depolarizing pulse of current injected through the intracellular recording micro-electrode (middle trace). Upper trace (dotted line) shows zero potential. *B*, current–voltage relationship measured with two intracellular electrodes. Current (50–200 msec pulses) was passed through one electrode (abscissa) and the steady-state voltage was recorded with the other electrode (ordinate). The input resistance was calculated by taking the slope at the linear part of the graph (arrow). In this example, the input resistance of the principal cell was 103 MΩ.

The current–voltage relationship of principal cells was measured by inserting separate recording and current-passing micro-electrodes into the cell body. Long current pulses (50–200 msec) were passed through one

electrode and the potential changes were measured with the other electrode. The membrane of principal cells was strongly rectifying when depolarized (Fig. 1*B*). The average input resistance of twenty-five neurones taken from the linear region of the slope of the steady state current–voltage relationship for hyperpolarizing potentials was 91 MΩ (the values varied greatly from cell to cell, with a range of 22–190 MΩ). The value in the undisturbed cell must normally be higher since insertion of two electrodes inevitably introduced an appreciable shunt to the membrane resistance. The mean time constant of the principal neurone was $10{\cdot}2 \pm 3{\cdot}5$ msec (data from ten cells). From these data and the measurement of the mean surface area of the principal cells given by McMahan & Purves (1976), the specific membrane capacitance was calculated to be 3·29 μF/cm^2 and specific membrane resistance was 3090 Ω cm^2.

However, evidence to be presented later (see page 441) indicates that the principal cells were electrically coupled to each other. Hence, the above value for input resistance includes a small contribution from the membrane resistance of adjacent neurones. Data presented in Table 3 suggest that this contribution introduced an error of about 7 %, so that the average membrane resistance of the principal cell is about 97 MΩ, the specific resistance 3306 Ω cm^2, and the specific membrane capacitance 3·06 μF/cm^2.

Membrane properties of interneurones. It was difficult to penetrate interneurones with micro-electrodes without damaging them, and consequently no data are available concerning their synaptic input and function. Usually, within seconds after inserting a micropipette, the cytoplasm and nucleus became very granular, the cell swelled, and the resting potential deteriorated. In a few instances, resting potentials as large as 60 mV were observed and action potentials could be evoked by passing current directly through the recording electrode (Fig. 2).

Vagal innervation of principal cells

A single threshold stimulus to the preganglionic nerve bundle typically evoked in the principal cells a large excitatory post-synaptic potential which generated an impulse (Fig. 3). As the stimulus strength was gradually increased and/or reversed, a second, third, and even a fourth increment in the size of the post-synaptic potential sometimes appeared, indicating that the neurones were innervated by more than one fibre (Fig. 4). The incidence of such multiple innervation varied greatly from animal to animal, but roughly 25 % of the cells (ten cells out of thirty-six in seven experiments) had two or more excitatory inputs when tested in this manner. This method of adjusting the stimulus strength and polarity in order to excite a single preganglionic fibre was used extensively in the following experiments.

Quantum content and preganglionic fatigue of vagal responses. As a first step in characterizing ganglionic transmission, it was of interest to establish the safety margin of vagal transmission and to determine the effects of frequency of preganglionic stimulation on the efficacy of transmission.

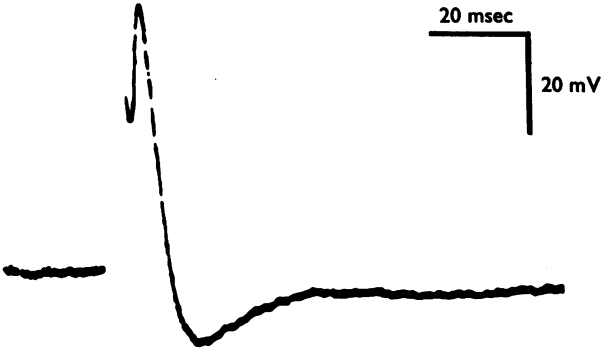

Fig. 2. An action potential in an interneurone, recorded intracellularly. Response to a 4 msec current pulse passed through the recording electrode. The stimulating pulse is brief and no current was passed while recording the impulse. The resting potential of this interneurone was 40 mV.

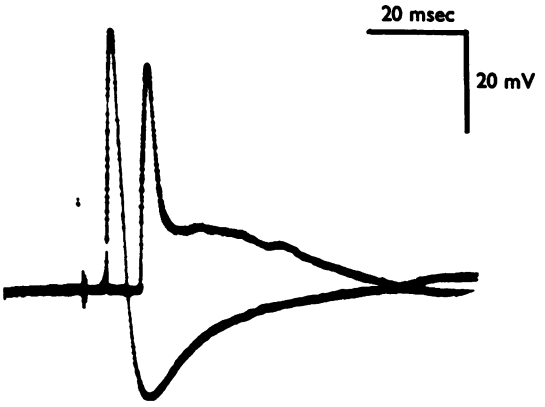

Fig. 3. Comparison of antidromic and synaptically evoked action potentials, recorded in the cell body of a principal neurone. The first impulse was evoked by stimulating the post-ganglionic trunk. The second response was evoked by stimulating the vagal stump. The latter, synaptically evoked, impulse is followed by a phase of prolonged transmitter action which shunts the action potential and reduces its size.

Repetitive stimulation of a single preganglionic fibre at a rate of 10–20/sec for prolonged periods (45–60 sec) reduced the rate of rise of the post-synaptic potentials, and at stimulation rates of 20/sec or greater the synaptic responses fell below threshold. If fatigued in this way, the sub-

threshold excitatory potentials fluctuated in discrete steps. This suggests that the fatigue was presynaptic in origin; that is, the quantal release of transmitter was reduced by repetitive stimulation (cf. Dennis *et al.* 1971). In addition, the frequency of spontaneous miniature e.p.s.p.s was increased after trains of stimuli, as in frog sympathetic ganglion cells (e.g. Blackman, Ginsborg & Ray, 1963*a*).

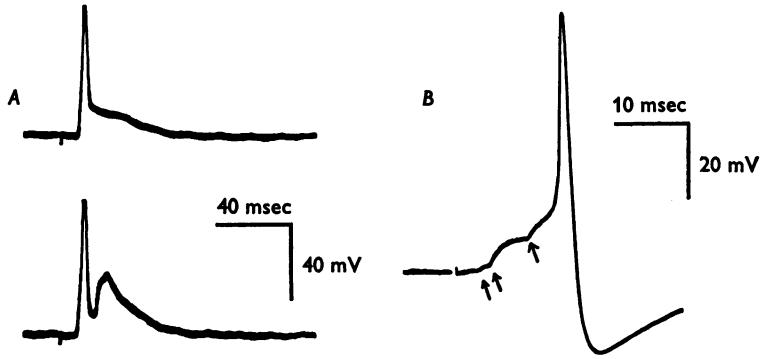

Fig. 4. Examples of two principal cells in the cardiac ganglion which are innervated by more than one preganglionic fibre. *A*, in one cell, threshold stimulation applied to the vagus stump evokes a large excitatory post-synaptic potential and an impulse (top trace). Stronger stimulation evokes a second response with longer latency (lower trace). *B*, in another principal cell three distinct increments in synaptic potentials with different latencies (arrows) are evoked by increasing the stimulus strength to the vagus nerve. Appropriate adjustments of stimulus strength and polarity could selectively excite each of these different inputs (not shown).

It was expected that vagal synapses liberated transmitter in a quantal fashion, in analogy with transmission at the nerve–muscle junction of skeletal fibres (Del Castillo & Katz, 1954), frog sympathetic ganglion cells (Blackman, Ginsborg & Ray, 1963*b*), and the cardiac ganglion of the frog (Dennis *et al.* 1971). The quantal nature of transmitter release was confirmed and the quantum content measured in the following experiments.

Because ganglion cells normally responded to stimulation of a single preganglionic axon with impulses which obscured the underlying vagal post-synaptic potential, the quantal content of the evoked synaptic response could not be analysed directly. Instead, an indirect method was used which compared the synaptic currents generated by preganglionic stimulation with the current generated by spontaneous miniature excitatory post-synaptic potentials. This method is described in the Appendix.

The results of these experiments showed that synaptic responses which were just at threshold were comprised of only about 8–9 quanta whereas,

on the average, 22–23 quanta were released by a single vagal stimulus. Table 1 summarizes these data. These findings indicate a large safety margin for impulse generation by vagal excitation.

Axon collateral synapses of principal cells

McMahan & Purves (1976) have shown that some nerve terminals remain on principal cells after preganglionic axons are severed and degenerate.

TABLE 1. Quantal content (m) of responses evoked by preganglionic stimulation. For evoked responses (second column) m was measured by stimuli applied every 2 sec (see Appendix). For threshold responses (third column) m was measured during repetitive stimulation at 20/sec or in the presence of 10 mM-$MgCl_2$. The 'safety factor' (last column) is the quantal content of the evoked response divided by that of the threshold response

Experiment	m, evoked response	m, threshold response	Safety factor
1	16·0	8·9	1·8
2	—	14·1	—
3	23·8	13·2	1·8
4	19·2	—	—
5	40·7	—	—
6	36·5	—	—
7	25·6	—	—
8	43·0	—	—
9	11·2	4·0	2·8
10	10·4	4·0	2·6
11	23·0	—	—
12	18·2	—	—
13	10·3	—	—
14	15·5	—	—
15	17·2	3·6	4·8
16	20·6	—	—
17	12·0	—	—
18	14·5	—	—
19	13·3	—	—
20	25·0	15·5	1·6
21	18·7	8·9	2·1
22	16·4	12·7	1·3
23	19·7	—	—
24	32·0	9·0	3·6
25	20·8	9·7	2·1
26	26·0 (dual innervation)	4·5	5·8
	30·2		6·7
27	13·5	3·0	4·5
28	24·6	—	—
29	28·0	—	—
30	37·3	—	—
31	36·2	7·2	5·0
Mean ± S.D.	22·6 ± 9·2	8·5 ± 4·2	3·3 ± 1·7

Furthermore, they found that these remaining terminals structurally resemble the excitatory cholinergic vagal synapses. A series of experiments were undertaken to test whether these synapses represented functional interconnexions between the cells in the ganglion.

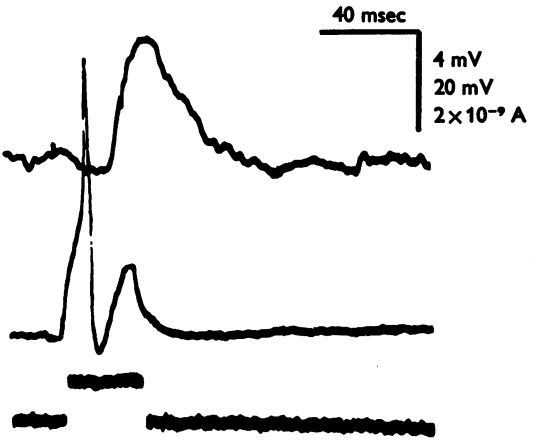

Fig. 5. Illustration of post-ganglionic axon collateral synapses between two principal cells. The neurones were impaled with intracellular microelectrodes. A 30 msec depolarizing current pulse (bottom trace) passed through the recording electrode triggered an action potential in one cell (middle trace). This, in turn, evoked an excitatory post-synaptic potential in the second principal cell (top trace). The upper response was caused by the impulse in the middle record since subthreshold depolarization of the one cell did not cause a response in the second cell.

The most direct way to demonstrate the presence of synaptic connexions between ganglion neurones was to impale a principal cell with a microelectrode, stimulate it by injecting intracellular depolarizing currents, and search for another principal cell in which responses could be recorded. Such synaptic interaction was successfully demonstrated in four experiments. Fig. 5 shows an example of the response in one principal cell (upper trace) evoked by suprathreshold current injected into a second principal cell (middle trace). The two neurones were not reciprocally innervated in any of these four cases; i.e. when cell *A* innervated cell *B*, no synaptic response occurred in the reverse direction. Further, direct stimulation of a single principal cell was never followed by a synaptic response in the same neurone.

The most likely explanation of these e.p.s.p.s is that they were produced by activation of principal cell axon collaterals which had been structurally identified by McMahan & Purves (1976). It seems reasonable to conclude, therefore, that these synapses were excited when a post-ganglionic axon propagated an impulse through a collateral branch to another ganglion cell.

Because it was rare to locate two principal cells which were connected by collateral synapses, alternative experiments were devised to study the collateral innervation of principal cells in greater detail. Vagal innervation of the ganglion was eliminated by cutting the preganglionic nerves and allowing the vagal terminals to degenerate (see Roper, 1976). Two weeks or more following this operation, it was not possible to evoke any synaptic responses by stimulating the degenerating distal vagal stump. On the other hand, stimulation of the post-ganglionic nerve trunk frequently

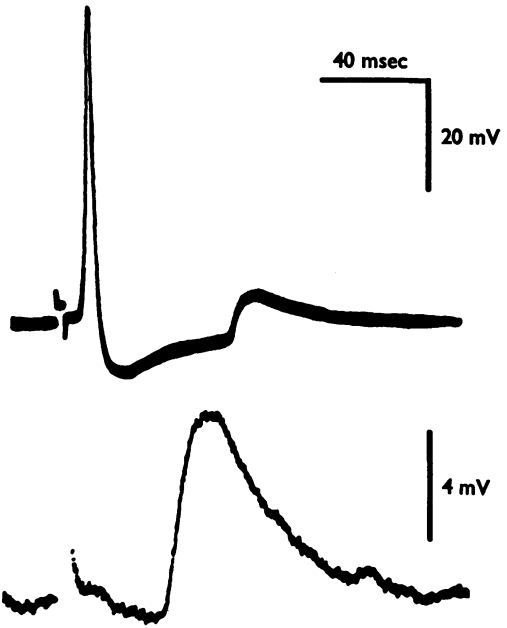

Fig. 6. Responses recorded in a principal cell caused by excitation of axon collateral synapses. The preganglionic nerve in this experiment had been cut 5 weeks before and the vagal terminals had degenerated. In the upper record, stimulation applied to the post-ganglionic trunk (artifact at beginning of record) evoked an antidromic impulse followed by an excitatory post-synaptic potential with longer latency. In the lower record, reversal of the stimulus polarity evoked the axon collateral response alone. The gain on the lower record has been increased.

evoked excitatory axon collateral potentials as well as antidromically conducted impulses, recorded intracellularly from principal cells (Fig. 6). These collateral responses typically were small and only occasionally reached threshold. The collateral synaptic potentials evoked by post-ganglionic stimulation in deafferented ganglia always appeared after the antidromic impulse if the latter was present (Fig. 6, top trace). By proper adjustment of post-ganglionic stimulation, collateral responses sometimes

were evoked alone (Fig. 6, bottom trace). In addition, spontaneous miniature e.p.s.p.s were recorded in roughly half the neurones in vagus-denervated ganglia, especially if the preparation was treated with potassium or lanthanum (see below). These spontaneous miniature potentials were about the same amplitude as those in normal ganglia which occurred after repetitive stimulation of the vagus nerves. Evoked and spontaneous synaptic potentials from axon collaterals were seen for as long as the operated animals were kept (10 weeks).

To exclude any extrinsic innervation that may have been overlooked (i.e. non-vagal) and to confirm further that these excitatory potentials were intrinsic to the ganglion, ganglia were excised from the animal and kept in sterile culture medium (Leibovitz medium, diluted to 80% and supplemented with Ca^{2+}, 2 mM final concentration, and glucose, cf. McMahan & Kuffler, 1971) at room temperature for up to 1 month. Under these conditions, extrinsic innervation degenerated within the first week and principal ganglion cells and cardiac muscle fibres survived well (see following paper). Even in the ganglia maintained *in vitro* for 2–3 weeks, stimulation of the post-ganglionic nerve evoked collateral synaptic responses (Fig. 7) similar in all respects to those recorded *in vivo* from intact and vagus-denervated ganglia.

Pharmacology of axon collateral synapses. It was expected that post-ganglionic axon collateral synapses were cholinergic since post-ganglionic parasympathetic innervation of the cardiac muscle fibres is cholinergic. Low concentrations of acetylcholine antagonists such as dihydro-β-erythroidine (10^{-8} to 10^{-7} g/ml.), curare (10^{-5} g/ml.), and hexamethonium (10^{-5} to 10^{-4} g/ml.) rapidly and reversibly blocked the post-ganglionic axon collateral responses. Fig. 8 compares the effects of dihydro-β-erythroidine on the synaptic responses evoked by preganglionic vagal stimulation and axon collateral stimulation in two different experiments. These findings suggest that the contralateral nerve endings, like the vagus nerve terminals and the post-ganglionic endings on the heart muscle, release acetylcholine.

Efficacy of post-ganglionic axon collateral innervation. The axon collateral synaptic responses typically were smaller than vagal excitatory potentials. The small size of axon collateral responses is attributed to a low quantum content (m) of collateral synaptic potentials compared with that of the vagal responses (see above), as determined by measuring the quantal composition.

Characteristically, excitation of a single collateral synapse produced responses which had a constant latency and which fluctuated in discrete amplitude steps with numerous failures (Fig. 9), similar to the end-plate potential at the neuromuscular junction in the presence of high Mg^{2+} and

low Ca^{2+} (Fatt & Katz, 1952; Del Castillo & Katz, 1954). It was possible to estimate the quantum content by taking the ratio of the average evoked response amplitude to the average size of the spontaneous miniature potentials (Del Castillo & Katz, 1954) or by techniques described in the Appendix. The quantum content was much less than that of the vagal response; m varied from less than 1 to about 5. This is illustrated by the

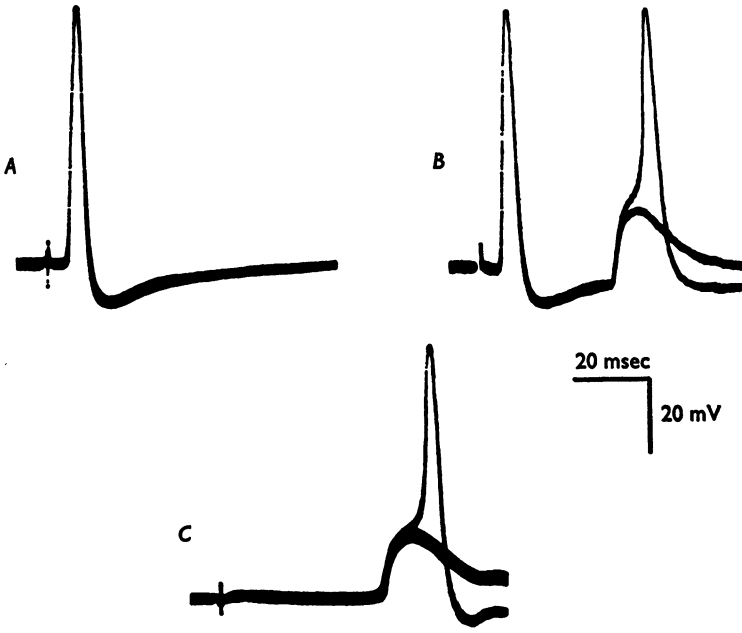

Fig. 7. Axon collateral responses in a ganglion cell which had been in organ culture for 20 days. All extrinsic innervation to the ganglion had degenerated, but post-ganglionic stimulation still evoked synaptic responses. *A*, superimposed traces of antidromically conducted action potentials caused by stimulating the post-ganglionic trunk. *B*, increasing the stimulus strength evoked excitatory post-synaptic potentials with longer latencies which occasionally reach threshold and trigger an impulse. *C*, reversing the polarity of the stimulus to the post-ganglionic trunk evoked axon collateral responses alone.

data taken from one experiment in a vagus-denervated ganglion; antidromic stimulation evoked fluctuating responses which varied from 2·1 to 5·4 mV with thirteen failures out of seventy trials. The average spontaneous miniature amplitude was 2·45 mV and the average response was 2·91 mV. Hence, for this particular experiment, the quantum content was 1·2. Insufficient data were collected to analyse the detailed mechanism of release (e.g. whether release obeyed Poisson statistics). Nevertheless, it is

clear that the quantum content of collateral responses is only a fraction of that of vagal responses and accounts for the smaller size of the former.

Distribution of axon collateral synapses. Several questions arise concerning the function of these collateral synapses. For example, how many principal cells receive collateral innervation and how many neurones innervate an individual principal cell? These questions were studied in preparations in

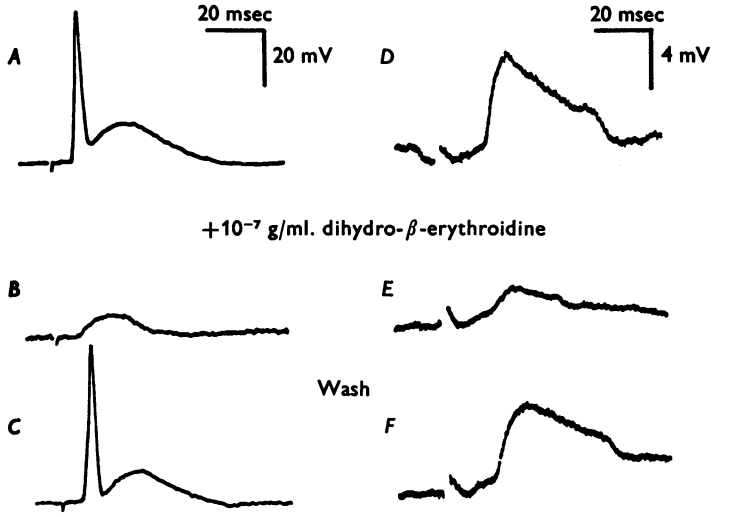

Fig. 8. Effect of a cholinergic antagonist, dihydro-β-erythroidine, on preganglionic responses (left traces) and post-ganglionic axon collateral responses (right traces). Two different experiments are shown. Responses evoked by stimulation of the preganglionic nerve in an intact ganglion are shown on the left. Responses evoked by post-ganglionic stimulation in a denervated ganglion are shown at the right. *A*, *D*, normal responses. *B*, *E*, responses after addition of dihydro-β-erythroidine (10^{-7} g/ml.). *C*, *F*, responses recorded after washing out the drug.

Fig. 9. Quantal fluctuations in axon collateral responses recorded intracellularly. Each record shows superimposed responses in one experiment evoked by suprathreshold stimuli applied to the post-ganglionic stump in a denervated ganglion. The response varies in quantal steps, with an occasional failure. The spontaneous excitatory potentials in this cell were the same size as the smallest evoked responses.

which the vagal innervation had degenerated. The collateral synapses were activated in two ways, by antidromic stimulation of the post-ganglionic nerve trunk and by increasing the frequency of spontaneous transmitter release. Antidromic stimulation evoked collateral responses in about half the cells. Normally there was a very low frequency of spontaneous miniature potentials (less than 1 per minute), but they were readily detected (up to about 0·1–0·5/sec) when the concentration of K^+ in the bath was raised to 15 mM (cf. Dennis *et al.* 1971) or when 0·1 mM-$LaCl_3$ was added to the bath for 5–10 min (cf. Heuser & Miledi, 1971). Again, in 50 % of the trials, spontaneous miniature potentials were observed after this treatment.

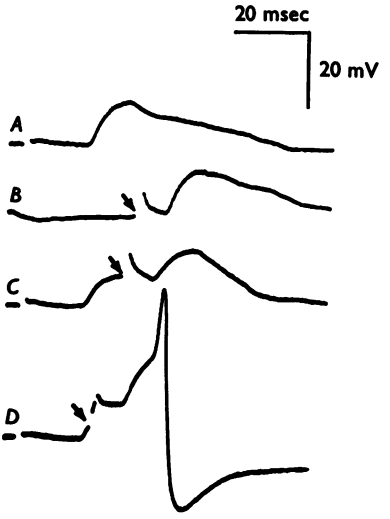

Fig. 10. Convergence of axon collateral synapses on to a single principal cell. The post-ganglionic nerve stump in a denervated ganglion was divided into two bundles; stimulation applied to either bundle evoked separate collateral responses with different latencies (*A*, *B*). When the two stimuli were paired at a 27 msec interval (*C*) the responses summed; if the interval was reduced, an impulse was generated (*D*). Arrows mark the artifact caused by the second stimulus.

Thus, spontaneous excitatory synaptic potentials and/or evoked responses were recorded in about half of the cells tested. This figure is an underestimate of the true value since not all the ganglion cell axons were activated by stimulation of the post-ganglionic bundle (i.e. it was not possible to excite antidromically all the ganglion cells) and it is difficult to detect reliably spontaneous potentials in all instances. However, it is clear that a large fraction of principal neurones are innervated by axon collaterals from other principal neurones.

Multiple innervation of principal cells by axon collaterals. Many principal cells received collaterals from more than one other principal cell. An example of such convergence is illustrated in Fig. 10. The post-ganglionic bundle was divided into two branches and each was drawn into a separate suction electrode for stimulation. The preganglionic nerves had been severed 3 weeks before in order to eliminate vagal terminals. Stimulation of either post-ganglionic branch evoked independent collateral responses with different latencies (Fig. 10*A*, *B*), which, when paired at an appropriate interval (Fig. 10*D*), generated an impulse.

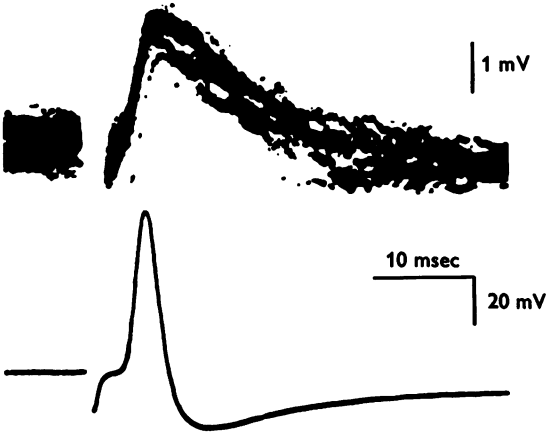

Fig. 11. Electrical synapses between principal neurones. Two adjacent principal cells were impaled with micro-electrodes. Antidromic stimulation evoked action potentials in one cell (lower trace) which are electrotonically conducted to the neighbouring cell (upper trace). Several records of the antidromic impulses and electrotonic responses are superimposed. The post-ganglionic nerve stump was stimulated at a rate of 50/sec which is sufficient to fatigue chemical synaptic responses in the ganglion.

Electrical synaptic connexions

Another response recorded in principal cells had several characteristics of electrical spread of impulses from neighbouring neurones. This was a brief depolarization of about 2 mV or less following antidromic post-ganglionic stimulation (Fig. 11). The response was not fatigued by high-frequency stimulation (up to 50/sec) or blocked by high-Mg^{2+} Ringer. The existence of electrical coupling between principal cells was confirmed in the following experiments.

Electrotonic transmission of steady-state potentials. Adjacent principal neurones were impaled with micro-electrodes in order to pass currents into one cell and search for electrotonic potentials in the other cell. In a few experiments it was possible to impale each cell with two micropipettes so

that intracellular currents could be passed and potentials measured independently. However, due to the difficulty of placing two electrodes in each cell, most experiments were conducted with recording and current-passing electrodes in one cell only with a single recording electrode in the adjacent neurone.

In the first series of experiments, long-duration (50–300 msec) current pulses were injected into one ganglion cell. The potential changes in that cell (v_1) and in the coupled neurone (v_2) were recorded simultaneously. The ratio of v_1 to v_2 gives the 'attenuation factor' (Furshpan & Potter, 1959). Fig. 12 shows a typical instance of electrical coupling; the hyperpolarizing potential generated by current-injection into one cell was transmitted to the second cell with an attenuation of fortyfold. Withdrawing the recording electrode from the second cell and repeating the experiment did not reveal any appreciable extracellular response.

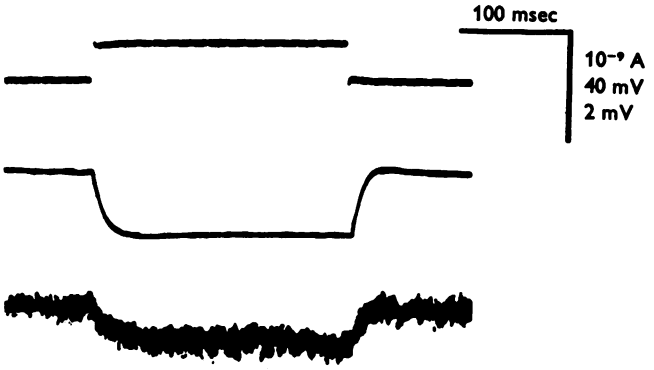

Fig. 12. Example of electrical coupling of long potential changes between principal neurones. Two juxtaposed ganglion cells were impaled with microelectrodes; a 240 msec hyperpolarizing current pulse (upper trace) was injected into one neurone via the recording electrode and caused a large response there (middle trace). A small fraction of that response is recorded in the adjacent principal cell (lower trace), due to electrotonic spread through specialized synaptic contacts.

In these experiments the potential changes in the first cell were varied over a wide range and were plotted against the attenuated responses in the neighbouring cell (Fig. 13). This relationship was always found to be linear. The attenuation factor was determined by calculating the slope of the regression line drawn through these points (e.g. Fig. 13). The average attenuation factor for these experiments with steady-state pulses was 11·25. Thus, about 9 % of the potential change in one neurone appeared in the coupled neurone. Data from additional experiments are presented in Table 2.

There was no evidence of rectification of the electrotonic transmission between ganglion cells. When the differences in the input resistances of the two coupled cells were taken into account (cf. Furshpan & Potter, 1959) it was shown that potential changes were transmitted equally in both directions across the electrical junctions (Fig. 13*A* and Table 3). Thus, the coupling resistance (R_s) for current flow between cells in either direction was not altered over a wide range of membrane voltages.

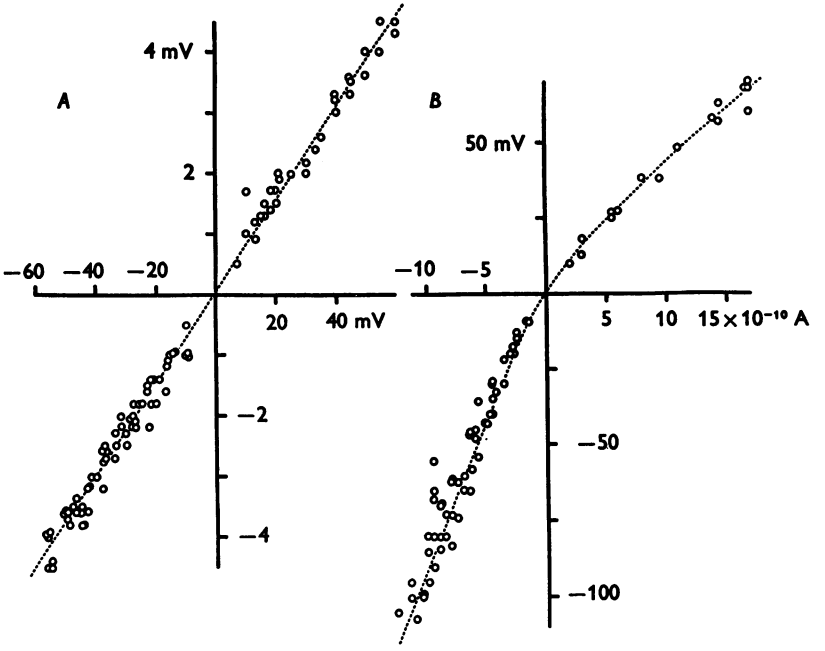

Fig. 13. Quantitative measurement of the electrical coupling between adjacent principal cells. Two micro-electrodes were inserted into each cell in order to pass current and measure potential changes independently. *A*, current injected into the first cell caused a voltage change in that cell (v_1) and an attenuated response in the second cell (v_2) and this is plotted in the graph on the left. The abscissa is v_1 and the ordinate is v_2. The slope of the regression line drawn through the points is the attenuation ratio (see text). *B*, the input resistance of the coupled cell was measured by passing current pulses (abscissa) and recording the potential changes (ordinate). This value is used to calculate the resistance of the electrical junctions, R_s.

Magnitude of the coupling resistance between principal neurones. The mean value of R_s determined from an initial series of experiments where the same micro-electrode in each cell was used to pass current and to record potentials was $7{\cdot}81 \times 10^8\ \Omega$. These measurements were repeated in three experiments where it was possible to penetrate each cell with a

recording and a current-passing micro-electrode. From these latter experiments a value for $R_s = 5{\cdot}45 \times 10^8\,\Omega$ was calculated, independent of the direction of current flow (Table 3).

TABLE 2. Quantitative measurement of electrical transmission between principal cells in the cardiac ganglion. The attenuation ratio (see text) for current pulses (column 3) is compared with the attenuation ratio for action potentials (column 4). Input resistance of the coupled cell, R_2 (column 5), was measured by plotting the current–voltage relationship (see text). The resistance of the electrical junction R_s (column 6) is given by $[v_1/v_2 - 1] \times R_2$ (cf. text). When possible, the transmission of current pulses and impulses was tested in both directions across the electrical junction (column 2). A Wheatstone-bridge circuit was used in order to apply current and measure potentials with the same intracellular electrode in at least one cell of each pair

Expt.	Coupling direction	Attenuation ratio, current pulses v_1/v_2	Attenuation ratio, action potentials V_1/V_2	Input resistance $R_2 \times 10^6\,\Omega$	Resistance of junctions, R_s $R_s \times 10^8\,\Omega$
1	—	31·5	166	50	15·25
2	—	16·8	—	—	—
3	*a b*	1·9	45	—	—
	b a	3·2	77	—	—
4	*a b*	1·5	—	80	0·40
	b a	3·5	17	63	1·58
5	—	7·7	70	—	—
6	—	3·6	—	—	—
7	*a b*	14·9	—	3	0·42
	b a	21·7	—	11	2·28
8	*a b*	28·8	—	46	12·79
	b a	8·4	—	33	2·44
9	*a b*	7·1	250	132	8·05
	b a	21·1	—	16	3·22
10	*a b*	10·9	166	190	18·81
	b a	9·4	46	250	21·00
11	—	5·4	—	—	—
12	—	1·9	—	—	—
13	*a b*	16·2	53	23	3·50
	b a	9·1	—	146	11·83
	Mean	11·2	98·9	80·2	7·81

The value for R_s was calculated by the expression $R_s = (v_1/v_2 - 1) \times R_2$ which is derived from inspection of Fig. 15. R_2 was taken as the input resistance of the coupled cell. This introduces an error due to the contribution of R_1 and R_s in parallel with R_2 when input resistance is measured by the current–voltage relationship in that cell alone. The magnitude of the error equating R_2 to the input resistance is determined largely by the size of R_s since it is much larger than R_1. This problem is discussed in detail in Furshpan & Potter (1959), pp. 315–316. When it was possible to make a thorough analysis of the current–voltage relations with independent

electrodes in each cell as in Table 3 (cf. Watanabe & Grundfest, 1961), it was found that the value of R_2 and hence R_s was approximately 7 % higher than when R_2 was approximated equal to input resistance. The corrected values for R_s are given in the last column in Table 3.

TABLE 3. Quantitative measurement of electrical synaptic transmission between principal cells as in Table 2, but with independent current-passing and recording electrodes inserted into each cell. Column 4, input resistance R_2, is the slope of the voltage–current relations in each cell, as in Table 2. The values in column 6, corrected R_s, are calculated by measuring the true value for R_2 for each cell, which is not identical to the input resistance (see text)

Experiment	Coupling direction	Attenuation ratio current pulses v_1/v_2	Input resistance, $R_2 \times 10^6\ \Omega$	Resistance of junction $R_s \times 10^8\ \Omega$	Corrected $R_s \times 10^8\ \Omega$
1	*a* *b*	13·0	51·5 (*b*)	6·18	6·7
	b *a*	30·9	22·6 (*a*)	6·76	7·0
2	*a* *b*	25·9	31·0 (*b*)	7·72	8·0
	b *a*	6·1	76·0 (*a*)	3·88	4·6
3	*a* *b*	10·6	40·0 (*b*)	3·84	4·2
	b *a*	17·9	26·0 (*a*)	4·39	4·6
	Mean	17·4	41·2	5·46	5·9

Electrotonic coupling of action potentials. As was expected, the coupling of action potentials across electrical junctions was less effective than transmission of steady-state pulses, due to the incomplete charging of the membrane capacitance of the coupled cell. Fig. 14 illustrates the transmission of 60 msec current pulses and of action potentials across the same electrical junction. In this instance, transmission of the action potential across the junction could not be detected above the base-line noise in the coupled neurone. In a series of thirteen experiments the attenuation factor for action potentials varied from 17 to 250 and was always considerably greater than the attenuation factor of steady-state potential changes across the same electrical junction (Table 2).

Fig. 15 summarizes these findings with a circuit diagram of two adjacent principal cells coupled by an electrotonic junction of resistance R_s. It is likely that R_s represents the gap junctions which are found between these neurones (McMahan & Purves, 1976).

Organization of electrically coupled cells in the ganglion. Principal neurones frequently are grouped in small clusters of three to six cells. Within a group, one or two of the cells formed electrical contacts with an adjacent neurone, but there was an equal number of principal cells within the group which were not coupled to neighbouring cells. It may be that

the remaining neurones made electrical synapses with cells which were out of the field of view, but in any case, it does not appear that every principal cell is electrotonically coupled directly to every adjacent neurone.

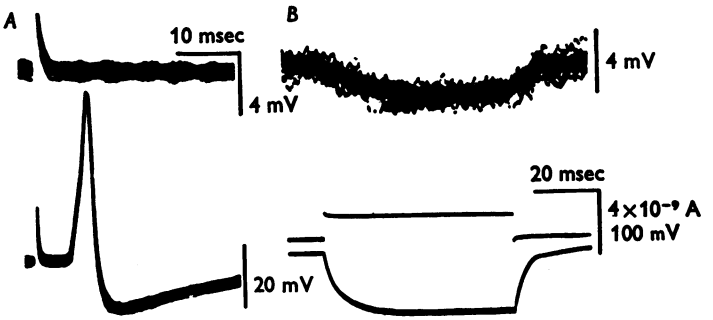

Fig. 14. Comparison of electrical coupling for long current pulses and for action potentials. Two adjacent principal cells were impaled with micropipettes. *A*, in the first cell, post-ganglionic stimulation evoked antidromically conducted responses (bottom trace) which did not produce detectable responses in the second cell (top trace). Several responses have been superimposed. *B*, direct hyperpolarization of the first cell with long pulses delivered through the recording electrode (bottom trace), however, is transmitted to the second cell (top trace) indicating that there was, in fact, electrical coupling between the nerve cells. The current pulse is shown in the middle trace of *B*.

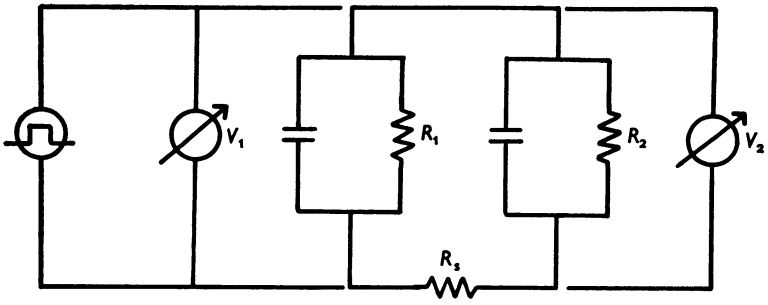

Fig. 15. Electrical circuit diagram representing the electrotonic coupling between principal neurones. Two nerve cells are represented by parallel resistance (R_1, R_2) and capacitance, and the cells are joined by an electrical junction, R_s. Current injected into Cell 1 (left) produces a potential change, V_1, in that neurone. A fraction of the current is transmitted to the second cell via R_s, and charges the resistance (R_2) and capacitance of the coupled cell to produce an attenuated response (V_2).

DISCUSSION

Organization of the mudpuppy cardiac ganglion

The focus of these studies has been the arrangement and properties of synaptic connexions in the ganglion. McMahan & Purves (1976) have demonstrated the existence of synapses which are intrinsic to the ganglion and of gap junctions between principal cells. The present electrophysiological studies have shown the presence of excitatory cholinergic axon collateral synapses and electrical junctions between principal cells. On the basis of known correlations between structure and function it seems likely that these correspond to the intrinsic synapses and gap junctions, respectively.

The functional organization of autonomic ganglia has received renewed interest subsequent to the discovery that complex synaptic potentials can be evoked in the superior cervical ganglia of rabbits (Eccles & Libet, 1961). These authors suggested that a great deal of synaptic interaction, involving both excitation and inhibition, occurs after preganglionic stimulation. The present investigation demonstrates that in parasympathetic cardiac ganglia also there are multiple sources of innervation, involving both chemical as well as electrical connexions. The organization of synaptic connexions in the mudpuppy cardiac ganglion is summarized in Text-fig. 13 of the preceding paper (McMahan & Purves, 1976).

The existence of post-ganglionic axon collateral synapses has not been demonstrated with certainty in autonomic ganglia of other species, although there have been reports which suggest that they occur in some mammals. Perri, Sacchi & Casella (1970) and, more recently, McLachlan (1974) were not able to find any electrophysiological evidence for intrinsic synapses which represent collateral innervation in intact superior cervical ganglia. On the other hand, Raisman, Field, Ostberg, Iverson & Zigmond (1974) found synapses in the rat superior cervical ganglion which persisted after complete preganglionic denervation and which did not arise from interneurones in the ganglion. They interpreted these as intrinsic noradrenergic synapses. In addition, Bunge, Rees, Wood, Burton & Ko (1974) and O'Lague, Obata, Claude, Furshpan & Potter (1974) report that dissociated superior cervical ganglion neurones from the rat are capable of forming synapses with each other in tissue culture. The findings presented here indicate that excitatory post-ganglionic axon collateral synapses may indeed be an important aspect of synaptic interaction within some autonomic ganglia *in vivo*.

It is worth while to comment on the fact that since principal cells in the mudpuppy innervate cardiac muscle as well as other principal cells, they provide an example of both excitation (collateral synapses) and inhibition

(cardiac muscle innervation) by the same neurone, and mediated by the same transmitter substance (cf. Kandel, Frazier & Coggeshall, 1967).

Quantum content of vagal innervation

The number of quanta released by a single preganglionic nerve in the mudpuppy ganglion varied from 10 to 43, with a mean value of 22·6. Most principal neurones received one afferent fibre and there was an average of 21–22 vagal boutons on each principal cell (McMahan & Purves, 1975). If there is equal probability for transmitter release from each preganglionic bouton, this suggests that each bouton released on the average about one quantum in response to a preganglionic volley.

The quantal content of evoked responses in the mudpuppy ganglion is similar to that in frog sympathetic ganglia (m = 6–34, Blackman, Ginsborg & Ray, 1963*a*) and in chick ciliary ganglia (m = 18–35, Martin & Pilar, 1964). However, the quantal content of responses in the mudpuppy is much less than that in toad sympathetic ganglia (m = 80–130, Nishi, Soeda & Koketsu, 1966) and greater than in guinea-pig superior cervical ganglia (m = 1·5, Sacchi & Perri, 1971). It would be of interest to know whether the variability in quantum content reflects a difference in the number and/or function of preganglionic boutons.

The post-synaptic response evoked by stimulating a single preganglionic fibre was large and the amount of transmitter liberated was 2–3 times greater than that needed for generation of an impulse (Table 1). It is interesting to compare the 'safety factor' at the cardiac ganglion with transmission at other synapses. For example, in lumbar sympathetic ganglia of the toad, the amount of acetylcholine released during normal transmission may be 2·5–8 times threshold amount (Nishi *et al.* 1966). On the other hand, the safety factor at the frog neuromuscular junction is smaller. Martin (1955) estimated that about 300 quanta are liberated at the end-plate. This represents only 1·5 times the number needed to generate an action potential if the quantum response is 0·5 mV, threshold is 44 mV, and summation of quanta is non-linear (Fatt & Katz, 1951; Martin, 1955). In mammalian autonomic ganglia the efficacy of an individual preganglionic input may be quite small. For example, in the guinea-pig superior cervical ganglion, a single preganglionic fibre releases only a fraction of the number of quanta necessary for excitation (Sacchi & Perri, 1971). This suggests that summation of preganglionic input is necessary for transmission in the guinea-pig ganglion.

Electrical coupling between principal cells

Gap junctions between principal cell bodies have been demonstrated in anatomical studies of the mudpuppy ganglion (McMahan & Purves, 1976)

and these presumably are the sites of electrotonic transfer studied in the present investigations. The presence of gap junctions at or near the cell body region simplifies the quantitative analysis of electrical coupling as no electrotonic decrement occurs between the micro-electrode and the electrical junction.

Although electrical coupling between neurones has not been previously reported in autonomic ganglia, the findings here suggest why they might not have been detected, if they occur. First, the electrical transmission of applied potential changes is weak and is highly dependent upon the input resistance of the coupled ganglion cell; even slight damage due to micro-electrode penetration readily shunts the small electrically coupled signals. In addition, brief signals, such as action potentials, are attenuated to an even greater extent than are steady-state pulses because of the time constant of the post-junctional membrane.

The functional significance of such low band-pass electrotonic coupling is not readily apparent. These junctions would be well suited for transmitting slow potential changes – for example, the slow synaptic potentials which are integral properties of synaptic transmission in other ganglia (Libet, 1970). However, no evidence for such slow synaptic potentials has been found in the cardiac ganglion of the mudpuppy.

Functional organization of the ganglion

There is no obvious explanation for the organization of synaptic inputs in the ganglion. It appears that the mudpuppy ganglion is not merely a relay station for the parasympathetic nervous system, but rather a site for more complicated synaptic interactions. One can hypothesize that the function of the axon collateral synapses is to augment and to prolong the output of the ganglion in response to a single preganglionic volley. This would tend to desynchronize any patterned input to the ganglion and produce a more sustained output. Because of the low quantum content of the post-ganglionic axon collateral responses, this recurrent synaptic excitation is not very powerful.

APPENDIX

When a single afferent axon to a principal neurone was stimulated by carefully adjusting the stimulus strength and polarity, a large excitatory post-synaptic potential was evoked which almost always generated an impulse. Because the impulse obscured the peak amplitude of the underlying post-synaptic potential, it was not possible to measure directly the quantal content, m, during the evoked responses. This Appendix describes a simple, though indirect, method for calculating the quantal content of

the vagus-evoked post-synaptic potential and describes experiments which confirm the validity of the method. A similar method has been reported by Blackman *et al.* (1963*a*).

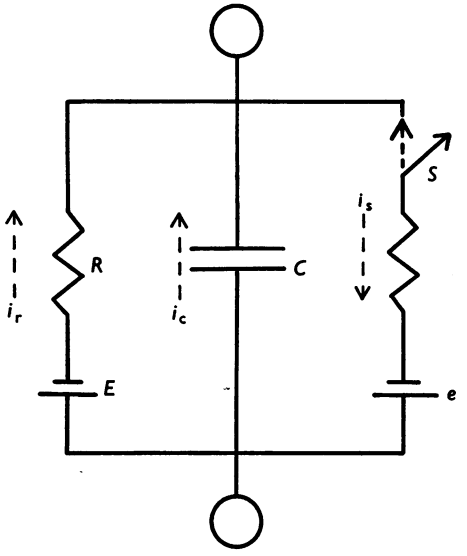

Fig. 16. Schematic diagram of a principal cell with chemical synapses located on the cell body. The input resistance (R) is in parallel with the membrane capacitance (C). Activation of synapses is represented by closing the switch (S). The resting potential is represented by a battery (E), as is the equilibrium potential for the chemical transmitter (e). i_c is capacitative current, i_r is restive current, i_s is synaptic current.

Principal neurones of the mudpuppy ganglion are roughly spherical and are devoid of dendrites. Hence, the soma can be represented by a simple electronic model, shown in Fig. 16. A synaptic potential is generated by closing the switch. It follows from this circuit that synaptic current $= i_r + i_c$ and that at or near the beginning of the response when the synaptic current (i_s) is greatest,

$$\begin{aligned} i_s &= i_c \\ &= C\,\mathrm{d}V/\mathrm{d}T. \end{aligned} \tag{1}$$

Therefore, the maximum synaptic current is proportional to the maximum rate of rise of the post-synaptic response since membrane capacitance, C, is constant.

It is assumed that the response of the principal cell to preganglionic stimulation consists of summed miniature potentials (see text). Hence,

the ratio of the maximum rates of rise of the evoked and miniature responses gives the quantum content (m) of the vagal response:

$$m = \frac{\mathrm{d}V/\mathrm{d}T_{\max}\ [\text{evoked response}]}{\mathrm{d}V/\mathrm{d}T_{\max}\ [\text{miniature response}]}. \qquad (2)$$

In these experiments, the signal recorded by the intracellular microelectrode was electronically differentiated and displayed with undifferentiated responses. It was nearly always possible to distinguish between the maximum rate of rise of the evoked post-synaptic potential and the start of the action potential, caused by vagal stimulation (Fig. 17*A*).

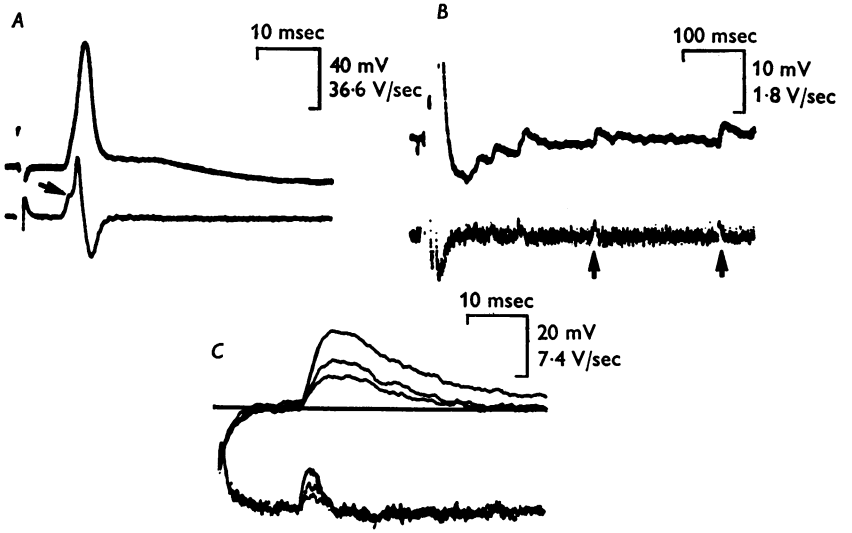

Fig. 17. Measurements of the quantal content of evoked responses in principal cells. In each record (*A*, *B*, *C*), the upper trace is the intracellular response (v) and the lower trace is the differentiated response ($\mathrm{d}v/\mathrm{d}t$). *A*, response to stimulation of a single afferent axon. The hump (arrow) on the differentiated trace is where $\mathrm{d}v/\mathrm{d}t$ for the underlying e.p.s.p. reaches a maximum. *B*, spontaneous miniature e.p.s.p.s caused by a brief train of stimuli applied to the vagal fibre. Sufficient time after the evoked responses was allowed for the potential to return to base line before miniature e.p.s.p.s were measured (arrows). *C*, synaptic responses to vagal stimulation in the presence of 10 mM-$MgCl_2$. Data such as these were used to construct the graphs shown in Fig. 18.

Miniature responses were produced by brief repetitive stimulation of the vagus nerve, which caused the appearance of spontaneous post-synaptic potentials (Blackman *et al.* 1963*a*) after the stimuli. Alternatively, the Mg^{2+} concentration in the Ringer was raised (up to 10 mM) and evoked responses were recorded. Under these conditions the evoked

response was depressed and fluctuated in discrete steps of amplitude with some failures. The smallest step in amplitude of the Mg^{2+} depressed evoked response was the same size as the spontaneous miniature e.p.s.p.s (1–5 mV). The miniature potentials were differentiated and displayed concurrently with the undifferentiated ones, as described above for the evoked responses. Values for m calculated in several experiments according to eqn. (2) are listed in Table 1.

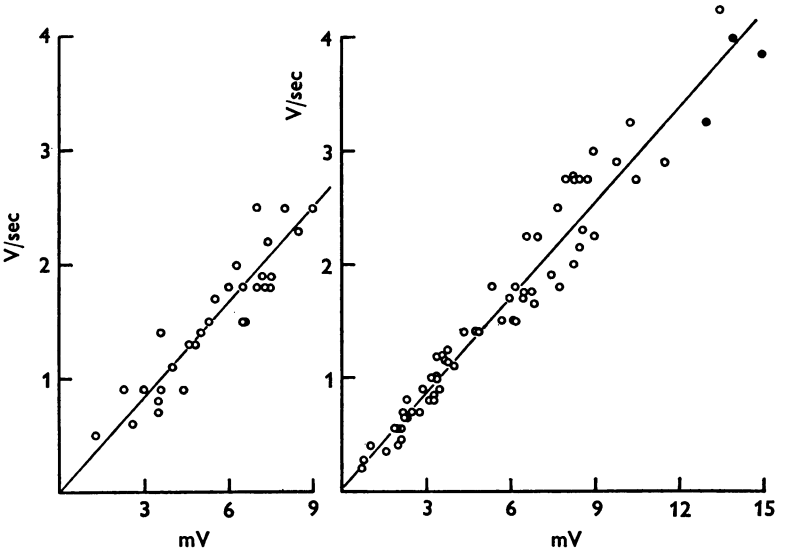

Fig. 18. Plot of differentiated responses (V/sec) *vs.* the amplitudes (mV) for synaptic responses evoked by vagal stimulation in the presence of elevated $MgCl_2$ (cf. Fig. 17*C*). Two different experiments are shown. Abscissae, maximum amplitude of evoked response (mV). Ordinates, maximum dv/dt of differentiated responses (V/sec). Lines were calculated by least-squares fit. Open circles, subthreshold responses. Filled circles, responses which were just at threshold for impulse generation.

To test the validity of the method, a comparison was made between the maximum rate of rise and the amplitude of subthreshold responses. A linear relationship would mean that quantal content measured by the present technique gives the same result as more conventional methods for subthreshold responses (Del Castillo & Katz, 1954), and by extrapolation, for suprathreshold responses. Fig. 18 illustrates results of two different experiments where dV/dT_{max} was plotted against maximum amplitude for a series of responses evoked in high magnesium. The graphs confirm that the maximum rate of rise (V/sec) is linearly related to the maximum amplitude (mV) for subthreshold responses, and that the line drawn

through the points passes through the origin. This comparison was nearly always found to be linear. In a few cases there was a slight upwards curvature to the graph which could be accounted for on the basis of non-linear summation of the quantal response amplitude (Martin, 1955).

These experiments confirm that quantal content of post-synaptic potentials can be measured simply and accurately in the principal cells of the mudpuppy ganglion by comparing the maximum rates of rise for evoked and for miniature responses.

I thank Dr S. W. Kuffler who participated in some of these experiments and who helped in preparing the manuscript. I also gratefully acknowledge the assistance of Drs U. J. McMahan, D. Purves, E. Furshpan, D. Potter and J. Diamond during the writing of the manuscript. I am indebted to the skilled technical help of Mr R. B. Bosler. Lastly, I would express my appreciation to the Edward Mallinckrodt, Jr. Foundation and the Colorado Heart Association for their financial support in the final stages of the experiments and preparation of the manuscript.

This work was supported by USPHS grants nos. 1 FO2 NS54024 and 1 RO1 NS 11505.

REFERENCES

BLACKMAN, J. G., GINSBORG, B. L. & RAY, C. (1963*a*). Spontaneous synaptic activity in sympathetic ganglion cells of the frog. *J. Physiol.* **167**, 389–401.

BLACKMAN, J. G., GINSBORG, B. L. & RAY, C. (1963*b*). On the quantal release of the transmitter at a sympathetic synapse. *J. Physiol.* **167**, 402–415.

BUNGE, R. P., REES, R., WOOD, P., BURTON, H. & KO, C.-P. (1974). Anatomical and physiological observations on synapses formed on isolated autonomic neurons in tissue culture. *Brain Res.* **66**, 401–412.

DEL CASTILLO, J. & KATZ, B. (1954). Quantal components of the end-plate potential. *J. Physiol.* **124**, 560–573.

DENNIS, M. J., HARRIS, A. J. & KUFFLER, S. W. (1971). Synaptic transmission and its duplication by focally applied acetylcholine in parasympathetic neurons in the heart of the frog. *Proc. R. Soc.* B **177**, 509–539.

ECCLES, R. M. & LIBET, B. (1961). Origin and blockade of the synaptic responses of curarized sympathetic ganglia. *J. Physiol.* **157**, 484–503.

FATT, P. & KATZ, B. (1951). An analysis of the end-plate potential recorded with an intra-cellular electrode. *J. Physiol.* **115**, 320–370.

FATT, P. & KATZ, B. (1952). Spontaneous subthreshold activity at motor nerve endings. *J. Physiol.* **117**, 109–128.

FURSHPAN, E. J. & POTTER, D. D. (1959). Transmission at the giant motor synapses of the crayfish. *J. Physiol.* **145**, 289–325.

HEUSER, J. & MILEDI, R. (1971). Effects of lanthanum ions on function and structure of frog neuromuscular junctions. *Proc. R. Soc.* B **179**, 247–260.

JACOBOWITZ, D. (1970). Catecholamine fluorescence studies of adrenergic neurons and chromaffin cells in sympathetic ganglia. *Fedn Proc.* **29**, 1929–1944.

KANDEL, E. R., FRAZIER, W. T. & COGGESHALL, R. E. (1967). Opposite synaptic actions mediated by different branches of an identifiable interneuron in Aplysia. *Science, N.Y.* **155**, 346–349.

KATZ, B. (1969). *The Release of Neural Transmitter Substances.* Springfield, Ill.: Thomas.

LIBET, B. (1970). Generation of slow inhibitory and excitatory post-synaptic potentials. *Fedn Proc.* **29**, 1945–1956.

MCLACHLAN, E. M. (1974). The formation of synapses in mammalian sympathetic ganglia reinnervated with preganglionic or somatic nerves. *J. Physiol.* **237**, 217–242.

MCMAHAN, U. J. & KUFFLER, S. W. (1971). Visual identification of synaptic boutons on living ganglion cells and of varicosities in postganglionic axons in the heart of the frog. *Proc. R. Soc.* B **177**, 485–508.

MCMAHAN, U. J. & PURVES, D. (1976). Visual identification of two kinds of nerve cells and their synaptic contacts in a living autonomic ganglion of the mudpuppy (*Necturus maculosus*). *J. Physiol.* **254**, 405–425.

MCMAHAN, U. J., SPITZER, N. C. & PEPER, K. (1972). Visual identification of nerve terminals in living isolated skeletal muscle. *Proc. R. Soc.* B **181**, 421–430.

MARTIN, A. R. (1955). A further study of the statistical composition of the end-plate potential. *J. Physiol.* **130**, 114–122.

MARTIN, A. R. & PILAR, G. (1964). Quantal components of the synaptic potential in the ciliary ganglion of the chick. *J. Physiol.* **175**, 1–16.

MATTHEWS, M. R. & RAISMAN, G. (1969). The ultrastructure and somatic efferent synapses of small granule-containing cells in the superior cervical ganglion. *J. Anat.* **105**, 255–282.

NISHI, S., SOEDA, H. & KOKETSU, K. (1966). Release of acetylcholine from sympathetic preganglionic nerve terminals. *J. Neurophysiol.* **31**, 114–134.

O'LAGUE, P. H., OBATA, K., CLAUDE, P., FURSHPAN, E. J. & POTTER, D. D. (1974). Evidence for cholinergic synapses between dissociated rat sympathetic neurons in culture. *Proc. natn. Acad. Sci. U.S.A.* **71**, 3602–3606.

PERRI, V., SACCHI, O. & CASELLA, C. (1970). Synaptically mediated potentials elicited by the stimulation of post-ganglion trunks in the guinea-pig superior cervical ganglion. *Pflügers Arch.* **314**, 55–67.

RAISMAN, G., FIELD, P. M., OSTBERG, A. J. C., IVERSON, L. L. & ZIGMOND, R. E. (1974). A quantitative ultrastructural and biochemical analysis of the process of reinnervation of the superior cervical ganglion in the adult rat. *Brain Res.* **71**, 1–16.

ROPER, S. (1976). The acetylcholine sensitivity of the surface membrane of multiply-innervated parasympathetic ganglion cells in the mudpuppy before and after partial denervation. *J. Physiol.* **254**, 455–473.

SACCHI, O. & PERRI, V. (1971). Quantal release of acetylcholine from the nerve endings of the guinea-pig superior cervical ganglion. *Pflügers Arch.* **329**, 207–219.

WATANABE, A. & GRUNDFEST, H. (1961). Impulse propagation of the septal and commissural junctions of crayfish lateral giant axons. *J. gen. Physiol.* **45**, 267–308.